Published in final edited form as:
J Am Chem Soc. 2013 May 29; 135(21): 7815–7818. doi:10.1021/ja4016815.

Silica encapsulation of fluorescent nanodiamonds for colloidal stability and facile surface functionalization

Ambika Bumb[†,‡], **Susanta K. Sarkar**[†,‡], **Neil Billington**[§], **Martin W. Brechbiel**[#], and **Keir C. Neuman**[†,*]

[†]Laboratory of Molecular Biophysics, National Heart, Lung, and Blood Institute, National Institutes of Health, 50 South Dr, Building 50 Room 3517, Bethesda, MD 20892, USA

[§]Cell Biology & Physiology Center, National Heart, Lung, and Blood Institute, National Institutes of Health, 50 South Dr, Building 50 Room 3525, Bethesda, MD 20892, USA

[#]Radiation Oncology Branch, National Cancer Institute, National Institutes of Health, 10 Center Drive, Building 10 Room 1B53, Bethesda, MD 20892, USA

Abstract

Fluorescent nanodiamonds (FNDs) emit in the near infrared and do not photo-bleach or photoblink. These properties make FNDs better suited for numerous imaging applications in comparison to commonly used fluorescence agents such as organic dyes and quantum dots. However, nanodiamonds do not form stable suspensions in aqueous buffer, are prone to aggregation, and are difficult to functionalize. Here, we present a method to encapsulate nanodiamonds with silica using an innovative liposome-based encapsulation process that renders the particle surface biocompatible, stable, and readily functionalized through routine linking chemistries. Furthermore, the method selects for a desired particle size and produces a monodisperse agent. We attached biotin to the silica-coated FNDs and tracked the three-dimensional motion of a biotinylated FND tethered by a single DNA molecule with high spatial and temporal resolution.

Fluorescent nanodiamonds (FNDs) are biocompatible nanoparticles with indefinite photo-stability[1]. Whereas organic dyes photobleach, quantum dots photoblink and have toxicity concerns, and gold nanoparticles exhibit weak size- and shape-dependent fluorescence, FNDs do not suffer from these non-ideal behaviors. Furthermore, their near infrared (NIR) fluorescence (~650 to 900 nm) makes them ideally suited for *in vivo* imaging[1]. The nitrogen-vacancy centers in these FNDs absorb broadly from 500 to 625nm and have a peak emission at 690nm (Figure S2). This is beneficial because in the NIR region the absorption of blood, water, and proteins is considerably smaller and, thus, light can penetrate tissue to depths of several centimeters[2,3]. Additionally, imaging agents in the NIR region minimize signal contamination from autofluorescence arising from intrinsic fluorophores that typically emit in the visible spectrum[4,5]. The large Stokes shift (>100nm) of FNDs affords further reduction in the autofluorescence background. However, biomedical applications of FNDs have faced two challenges due to the inherent properties of the material: 1) aggregation that leads to precipitation and 2) difficulty in functionalizing the inert diamond surface.

Corresponding Author neumankc@mail.nih.gov.
[‡]**Author Contributions**
A.B. and S.K.S. contributed equally.

ASSOCIATED CONTENT
Supporting Information
Figure equations, and experimental details. This material is available free of charge via the Internet at http://pubs.acs.org.

Biofunctionalization of FNDs can be achieved by noncovalent adsorption through weak interactions, such as hydrogen bonding, electrostatic forces, π-π stacking, van der Waals forces, and hydrophobic and hydrophilic interactions[7]. However, more stable and specific bonds are created by covalently linking FNDs to the desired biomolecule. Several methods of introducing functional groups to diamond surfaces have been described[8]. One drawback of some of these techniques is that they require surface modification of the diamond followed by functionalization. This can be an incomplete process and, particularly for the case of detonation diamonds, the precise nature and constituents of the surface may not be well defined[9].

Silica coating can assist in maintaining the stability of particle suspensions over a range of pH or electrolyte concentrations due to silanol groups that render the surface lyophilic[10]. Silica-coated material is dispersible in aqueous and non-aqueous solutions and is resistant to swelling with changes in solvent polarity. It is resistant to microbial attack, non-toxic, and biocompatible[11,12]. Additionally, silica is optically transparent[13], allowing efficient transmission of excitation and emission light. Finally, the surface silanol groups readily react with alcohols and silane coupling agents[14] affording covalent bonding with a variety of ligands, including targeting agents such as antibodies and peptides, as well as sugars and nucleotides.

To overcome the difficulties of functionalizing FNDs, we developed a liposome-based encapsulation process to trap nanodiamonds in a shell of silica (Figure 1a). This encapsulation rendered the FNDs biocompatible, stable, and easily modified through additional conjugation reactions. In addition, the method self-selects for a desired size and produces a monodisperse agent. Coated FNDs exhibited dramatically different properties than uncoated FNDs. Most noted was their improved colloidal stability. Uncoated FNDs rapidly precipitated out of solution (Figure 2a and Figure 2b), whereas coated FNDs have remained in solution for months. Characterizing particle size and surface charge is essential for understanding how to attach particles to surfaces as well as for predicting how an agent will behave *in vivo*. As shown in Figure 2, uncoated type 1b FNDs had large hydrodynamic diameters and low surface charge for pH values below 5 (Figure 2c and d). When the surface charge of a particle is low, electrostatic repulsion is not sufficient to prevent the particles from aggregating and flocculating, so the hydrodynamic diameter and polydispersity index (PDI), an indicator of aggregation, increase. For uncoated FNDs, the PDI was above 0.5, and reached the maximum of 1 for pH values below 10, indicating that the diamonds were polydisperse and aggregation was occurring.

The coated FNDs, on the other hand, were monodisperse with PDI values below 0.2, particularly in the pH range above 3 where a strong negative zeta potential (−35mV) allowed the particles to remain in colloidal suspension with a hydrodynamic diameter of ~45nm. Thus, encapsulating the FNDs with silica made them anionic, stable and monodisperse across the working pH range (5–8), as compared to uncoated FNDs. The coated FND's negative charge over the physiological pH range of 6–7 is desirable because it mimics the negative charge of most biomolecules[15], ideal for biomedical applications. Silica coating of the FNDs was confirmed by FTIR analysis (Figure 2e and 2f). The FTIR absorption spectra displayed characteristic silica bands between 800 and 1260 cm^{-1} corresponding to the superimposition of multiple SiO_2 and Si–OH peaks[6]. The strong absorption bands at 1090 and 950 cm^{-1} correspond to the asymmetric vibrations of Si–O and Si–OH, respectively. The same encapsulation process was tested with four different types and sizes of nanodiamonds obtained from various sources. Similar results were found with each, indicating that the method is applicable broadly regardless of the type of diamonds.

The second reason for encapsulating FNDs with silica was to facilitate the attachment of ligands enabling specific targeting of the FNDs. Silica is easily functionalized by silane-coupling agents containing a functional group that can be used for covalent attachment, i.e. an amine that can react with NHS esters or isothiocyanates (Figure 1b). As a proof of principle, an amine-reactive biotin moiety was conjugated to the silica-coated FNDs using 3-aminopropyltriethoxysilane (APTES) as an intermediate linker. The amine group was reacted to the biotin and the three ethoxysilane groups attached to the silanol groups of the encapsulated particle by the Stöber reaction[16] (Figure 1b).

Biotinylation of FNDs was tested at the single-molecule level using a prism-type total internal reflection fluorescence microscope (TIRFM) (Figure 3a) to quantify the specific binding of the FNDs to a surface passivated with polyethylene glycol (PEG) sparsely labeled with streptavidin (Supporting Information). On these surfaces the binding of the biotinylated silica-coated FNDs was ~15-fold greater than the non-biotinylated silica-coated FNDs (Figure 3). This demonstrates that the coated FNDs were successfully biotinylated and provides additional evidence that the FNDs were encapsulated with silica, which is required for the biotin linking chemistry.

The unique optical properties of FNDs, combined with the robust encapsulation and labeling scheme we have developed, make them almost ideal single-molecule tracking probes. We demonstrate this potential by measuring the three-dimensional (3-D) motion of a single FND tethered by a DNA molecule with high temporal and spatial resolution over an extended period of time. Tethered particle motion (TPM) of beads attached to DNA or RNA molecules is a robust and sensitive single-molecule method to study the physical properties of nucleic acids and their interactions with proteins[17,18]. In contrast to force-based methods such as optical and magnetic tweezers, and atomic force microscopy, TPM affords single-molecule measurements of physical properties and interactions in the absence of applied force. The results of 3-D TPM measurements of a 1.4 μm DNA molecule with a silica-coated and biotinylated ~30 nm diameter FND attached to the free end via a biotin–streptavidin linkage are shown in Figure 4. A prism type TIRF microscope was used to record the FND fluorescence for ~1 hour with 30 ms time resolution and ~20–70 nm spatial resolution (Supporting Information). Background fluorescence in the field of view was eliminated by photo-bleaching the observation area prior to tracking the FND, which does not photo-bleach. Motion in the plane (*x* and *y*) was tracked with a Gaussian localization tracking routine[19], whereas out of plane motion (*z*) was tracked by relating the position of the FND relative to the slide surface to the fluorescence intensity, which decreases exponentially in proportion to the evanescent excitation field (Supporting Information). Probability distributions of *x*- and *y*- positions are well described by the Gaussian Random Walk (GRW)[20,21] model (Figures 4e and f). The probability distribution of *z*-positions reflects the restricted motion of the FND due to the surface (Figure 4g). The *z*-position probability distribution is well described by a difference of two Gaussians, which is predicted in the long chain limit of the GRW[22]. With a contour length, L=1.4 μm, fits to three distributions (Figure 4e, 4f, and 4g) returned an average persistence length (l_p) of 55±6 nm, consistent with the accepted DNA persistence length.

Due to the small size of the FND relative to the characteristic length scale of the DNA, ($\sim \sqrt{Ll_p}$), we expect that the dynamics of the DNA were minimally influenced by the FND. More precisely, the excursion number defined by $N_r = r(Ll_p/3)^{1/2}$ where r is the radius of the particle, provides a measure of the influence of the particle on the dynamics of the polymer tether[21]. For $N_r < 1$ the dynamics are dominated by the DNA tether, whereas for increasing values of $Nr \geq 1$ the particle increasingly influences the motion[21]. For the silica-coated ~30 nm diameter FND and 1.4 μm DNA tether, the excursion number is 0.09. Indeed, for 30 nm

diameter FNDs, the excursion number is unity for a contour length of ~14 nm (~40 base pairs) assuming a DNA persistence length of 50 nm. Therefore, FNDs provide a suitable tracking probe for studying the dynamics of polymers such as DNA with short contour lengths. Along with being minimally perturbative, TPM tracking of FNDs in the evanescent field affords low background while providing a sensitive measure of *z* motion (Figure 4). Z-tracking is difficult in traditional bead-based TPM measurements, but has been achieved with specialized evanescent dark field scattering measurements with colloidal gold particles[20]. TPM measurements using FNDs share the advantages of small radius, high temporal and spatial resolution, long-term photo-stability, and straightforward *z*-motion tracking afforded by laser scattering from gold nano-particles, but can be performed on a standard TIRF microscope and do not suffer from the technical challenges associated with detecting weak scattered light[20]. These measurements demonstrate that functionalized FNDs can be used as sensitive and photostable probes for tracking 3-D motion of biomolecules with high spatial and temporal resolution.

In summary, we present a simple and robust method to encapsulate nanodiamonds with silica. The encapsulation process can be readily used to stabilize and functionalize any nanodiamond with a thin silica shell independent of the surface properties of the particle. Once encapsulated with silica, the particles are readily further modified through established silica functionalization schemes. We demonstrate the utility of this approach by covalently attaching biotin to FNDs and tracking the 3-D motion of a single biotinalyted FND attached to an individual DNA molecule with high spatial and temporal resolution over an extended period of time. Optically superior, stable, and functionalizable FNDs have a plethora of applications in the fields of nanotechnology and nanomedicine. For instance, silica-coated FNDs can be functionalized for multi-modal imaging with radio-labels and MRI contrast agents for targeted drug delivery with tracking ability. At the single-molecule level, they can be used to track labeled biomolecules over extended periods of time, and due to their wide excitation spectra, they can be used as stable fiducial markers for ultra-high resolution microscopy across multiple wavelengths. The energy level structure and electron spin coherence of FNDs also facilitates applications in ultra-low magnetic field detection and ultra-sensitive NMR[23–25]. Therefore, the ability to coat with silica and functionalize FNDs provides a unique nanomaterial for wide range of biological imaging applications.

Supplementary Material

Refer to Web version on PubMed Central for supplementary material.

Acknowledgments

This research was supported by the National Institutes of Health (NCI & NHLBI). We thank Joe Barchi for help with FTIR, the NHLBI Biophysical Core Facility and Grzegorz Piszczek for help with scattering measurements, and Jonathan Silver for help in preparing the DNA molecules. We thank Richard Leapman and Maria Aronova at NIBIB for assistance and Gopalakrishnan Balasubramanian for helpful discussions.

References

1. Yu SJ, Kang MW, Chang HC, Chen KM, Yu YC. Journal of the American Chemical Society. 2005; 127:17604. [PubMed: 16351080]
2. Bumb A, Regino C, Perkins M, Bernardo M, Ogawa M, Fugger L, Choyke P, Dobson P, Brechbiel M. Nanotechnology. 2010; 21:175704. [PubMed: 20368682]
3. Grosenick D, Wabnitz H, Rinneberg HH, Moesta KT, Schlag PM. Appl Opt. 1999; 38:2927. [PubMed: 18319875]
4. Andersson-Engels SW, BCJ. Cell Pharmacol. 1992; 3:48.
5. Weissleder R. Nature biotechnology. 2001; 19:316.

6. Beganskienė A, Sirutkaitis V, Kurtinaitiene M, Juškėnas R, Kareiva A. Materials Science. 2004; 10:287.
7. Xing Y, Dai L. Nanomedicine. 2009; 4:207. [PubMed: 19193186]
8. Mochalin VN, Shenderova O, Ho D, Gogotsi Y. Nat Nano. 2012; 7:11.
9. Kuznetsov O, Sun Y, Thaner R, Bratt A, Shenoy V, Wong MS, Jones J, Billups W. Langmuir. 2012; 28:5243. [PubMed: 22360371]
10. Mulvaney P, Liz-Marzan L, Giersig M, Ung T. J Mater Chem. 2000; 10:1259.
11. Jin Y, Kannan S, Wu M, Zhao JX. Chemical research in toxicology. 2007; 20:1126. [PubMed: 17630705]
12. Xue Z, Liang D, Li Y, Long Z, Pan Q, Liu X, Wu L, Zhu S, Cai F, Dai H. Chinese Science Bulletin. 2005; 50:2323.
13. Liu DM, Chen I. Acta materialia. 1999; 47:4535.
14. Ulman A. Chemical reviews. 1996; 96:1533. [PubMed: 11848802]
15. Vroman L. Science (New York, NY). 1974; 184:585.
16. Stöber W, Fink A, Bohn E. Journal of colloid and interface science. 1968; 26:62.
17. Dunlap, D.; Zurla, C.; Manzo, C.; Finzi, L. Single Molecule Analysis. Peterman, EJG.; Wuite, GJL., editors. Vol. 783. Humana Press; 2011. p. 295
18. Schafer DA, Gelles J, Sheetz MP, Landick R. Nature. 1991; 352:444. [PubMed: 1861724]
19. Sarkar, Susanta K, Marmer B, Goldberg G, Neuman Keir C. Current Biology. 2012; 22:1047. [PubMed: 22578418]
20. Lindner M, Nir G, Medalion S, Dietrich HRC, Rabin Y, Garini Y. Physical Review E. 2011; 83:011916.
21. Segall DE, Nelson PC, Phillips R. Physical review letters. 2006; 96:88306.
22. Blumberg S, Gajraj A, Pennington MW, Meiners JC. Biophysical journal. 2005; 89:1272. [PubMed: 15923224]
23. Balasubramanian G, Chan I, Kolesov R, Al-Hmoud M, Tisler J, Shin C, Kim C, Wojcik A, Hemmer PR, Krueger A. Nature. 2008; 455:648. [PubMed: 18833276]
24. Epstein R, Mendoza F, Kato Y, Awschalom D. Nature Physics. 2005; 1:94.
25. Takahashi S, Hanson R, van Tol J, Sherwin MS, Awschalom DD. Physical review letters. 2008; 101:047601. [PubMed: 18764365]

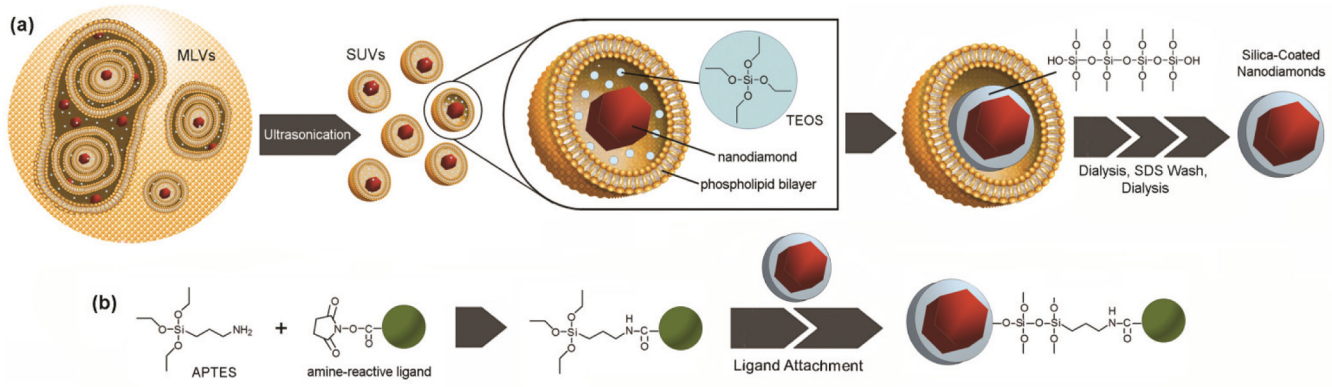

Figure 1.

(a) Nanodiamonds in a solution of TEOS are trapped in phospholipid POPC multilaminar vesicles (MLVs) that can range in size from 500–10000 nm. Ultrasonication breaks the MLVs into small unilamellar vesicles (SUVs) of nominally ~100 nm diameter. TEOS is converted into silica, catalyzed by TEA. Thereafter, free TEOS and TEA are dialyzed away. An SDS wash breaks up the liposomes to free the coated diamonds and the remaining reagents (i.e. SDS and POPC) are removed by dialysis. The final product is stabilized and monodisperse silica-encapsulated nanodiamonds. (b) Since the surface of the silica-encapsulated diamonds presents free silanol groups, a variety of silane agents can be used to attach biomolecules to the encapsulated diamonds. One such method is to conjugate a ligand to the amine group of APTES and use its remaining silanol groups to conjugate the ligand to the particle.

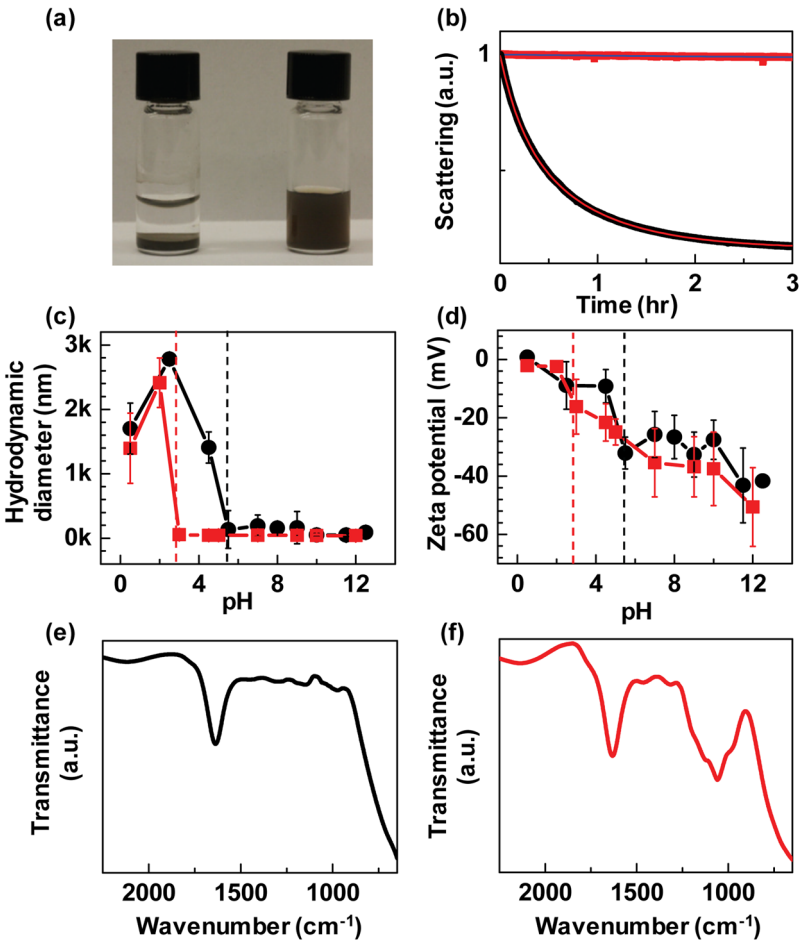

Figure 2.

(a) Uncoated diamond in water (left vial) and silica-coated diamond in water (right vial). (b) Settling of uncoated (black circles) and silica-coated diamond (red squares) measured by light scattering. Samples were excited at 635 nm and scattering was measured at 90° relative to excitation. Settling of coated diamond was fit to a single exponential with an offset (blue line), $I(t) = a_0 + a_1 \exp(-t/t_1)$. Fit parameters: $a_0 = 0.9784 \pm 0.0006$ a.u., $a_1 = 0.0220 \pm 0.0005$ a.u., $t_1 = 4.20 \pm 0.15$ hr, which we interpret as a majority (98%) stable component and a minority (2%) component that settles out slowly with a time constant of 4 hours. Error bars are the standard error of the fit. Settling of uncoated diamond was best fit to a double exponential with an offset (red line), $I(t) = a_0 + a_1 \exp(-t/t_1) + a_2 \exp(-t/t_2)$. Fit parameters: $a_0 = 0.1635 \pm 0.0001$ a.u., $a_1 = 0.5534 \pm 0.0010$ a.u., $t_1 = 0.7866 \pm 0.0012$ hr, $a_2 = 0.2786 \pm 0.0010$ a.u., $t_2 = 0.2189 \pm 0.0007$ hr. The low values of a_0 and time constants indicate that the majority (83%) of the uncoated diamonds precipitate in less than an hour. (c) The hydrodynamic diameter (Z-avg) and (d) zeta potential of silica-coated (red) and uncoated (black) nanodiamonds as a function of pH. At pHs below the dotted lines, the absolute value of the zeta potential was less than 20 mV and flocculation with increased size was observed. Error bars are 1 standard deviation. (e) FTIR spectrum of uncoated FND. (f) FTIR spectrum of silica-coated FND. Characteristic SiO_2 bands between 800 and 1260 cm^{-1}, the Si–O band at 1090 cm^{-1}, and the Si–OH band at 950 cm^{-1} are apparent in the spectra. In both the coated and uncoated ND samples, water was present. The band at 1635 cm^{-1} is due to the scissor bending vibration of molecular water[6].

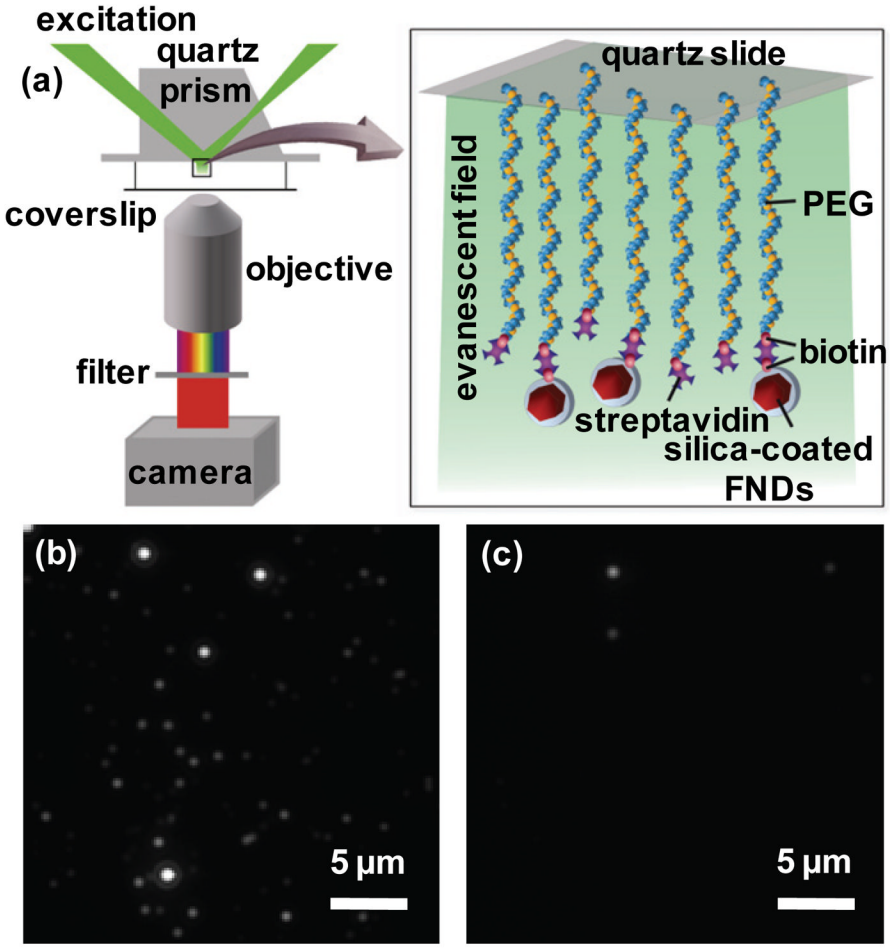

Figure 3.

(a) Schematic of single-molecule binding experiment. A quartz slide passivated with biotinylated PEG was saturated with streptavidin. Biotinylated FNDs were flowed into the flow cell and specific attachment to streptavidin-biotin-PEG was probed by comparing the number of bound particles before and after washing to remove non-specifically bound particles. FNDs were excited by the evanescent field (green) in a prism-type TIRFM (Supporting Information). (b) 60% of biotinylated silica-coated FNDs and (c) 4% of non-biotinylated silica-coated FNDs remained attached to the surface after the stringent acid-base wash. (Additional information in Figure S1.)

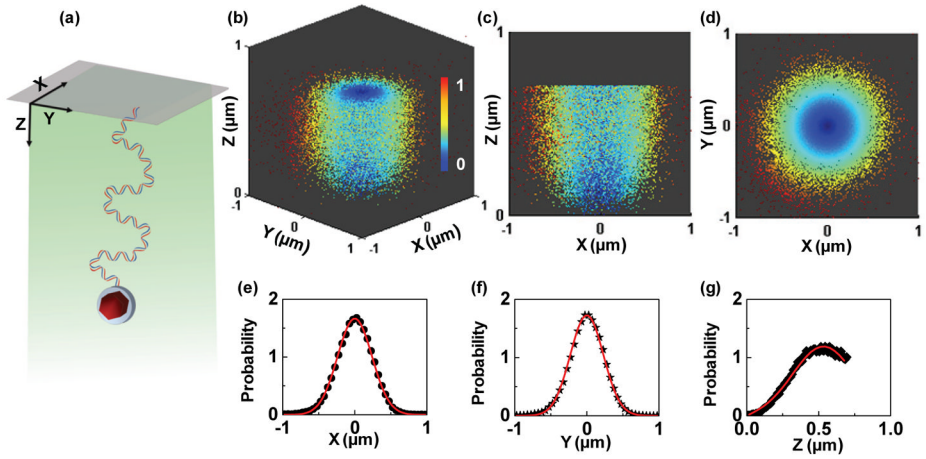

Figure 4.

Three dimensional tethered particle tracking (TPM) of DNA conformations using biotinylated FNDs. (a) One end of a 1.4 μm double-stranded DNA molecule is tethered to a quartz slide, while the other end is attached to a biotinylated ~30 nm FND. The FND is excited by the evanescent wave created at the interface of the quartz slide and buffer in the flow cell in a prism-type TIRFM. The evanescent field (green) decreases exponentially away from the quartz-buffer interface. Custom tracking software was used to track the *x*-, and *y*-positions, and the intensity (I) of the FND. The natural logarithm of the intensity provides a measure of the *z* -position as the FND moves in the exponentially varying evanescent field. An intensity threshold was used to avoid tracking errors, which resulted in missing positions of the FND at large *z*-extension and led to the flat tops in the distributions in (b) and (c). (b) Scatter plot of *x*-, *y*-, and *z*- coordinates of the tethered FND (n = 54,263), where $z = 0$ denotes the maximum of the intensity, which we assume was the quartz-buffer interface. Figures (b), (c) (side view of (b)), and (d) (top view of (b) are color-coded according to $r^2 = x^2 + y^2$, where r=0 is blue and r=1 is red. (e), (f), (g), The area-normalized probability densities along *x* (black circles), *y* (black stars), and *z* (black diamonds) (See SI). Average DNA persistence length obtained from fits to the distributions is 55 ± 6 nm (standard deviation). Cut-off in the *z*-distribution corresponds to the intensity threshold used in the tracking software.